Cell Reports, Volume *31*

Supplemental Information

Epigenomically Bistable Regions across Neuron-Specific Genes Govern Neuron Eligibility to a Coding Ensemble in the Hippocampus

Shannon C. Odell, Faten Taki, Shifra Liba Klein, Rosa J. Chen, Olivia B. Levine, Mary Jane Skelly, Anika Nabila, Elizabeth Brindley, Judit Gal Toth, Friederike Dündar, Caroline K. Sheridan, Robert N. Fetcho, Alicia Alonso, Conor Liston, Dan A. Landau, Kristen E. Pleil, and Miklos Toth

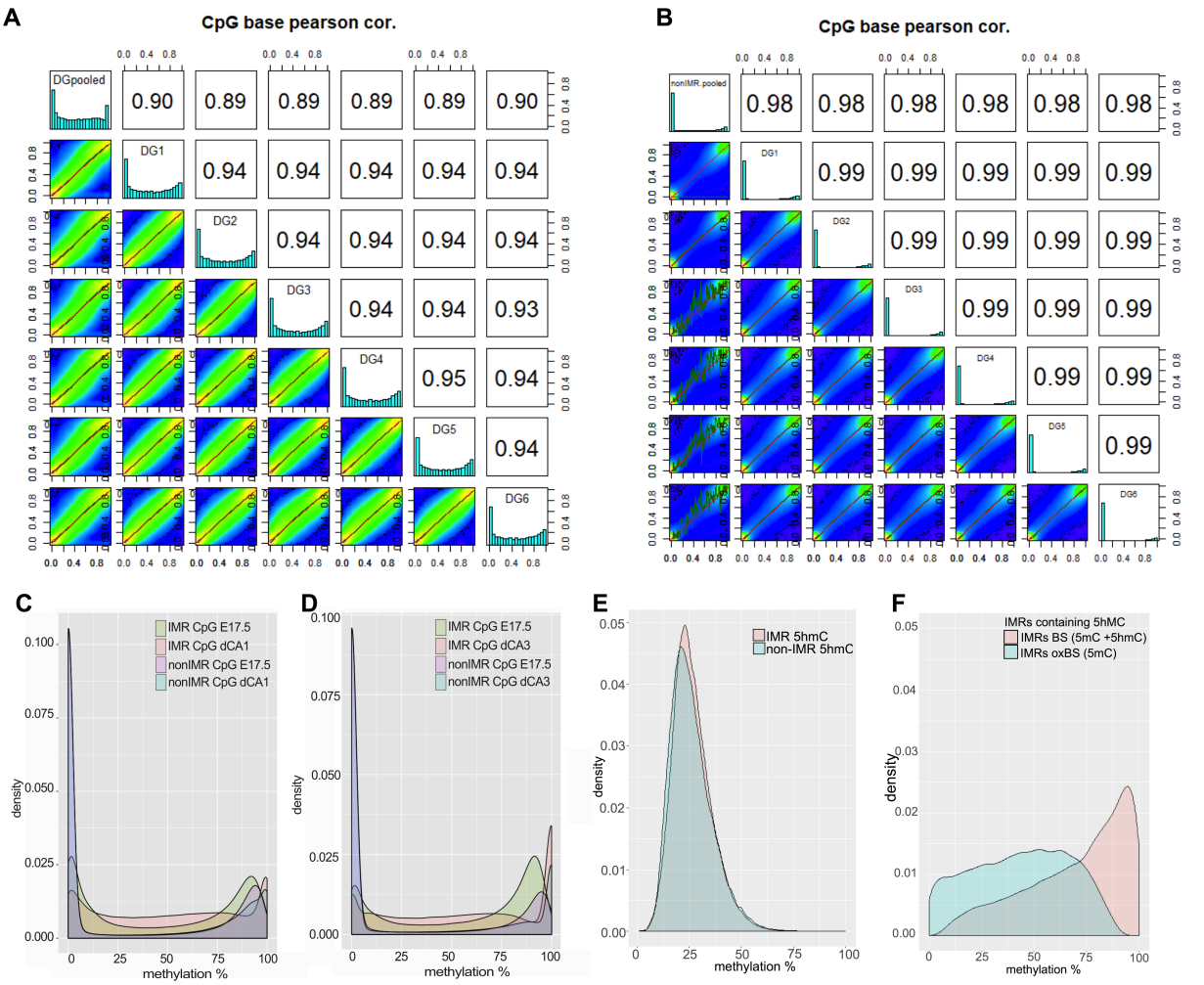

Supplemental Figure S1: Characteristics of IMRs. Related to Figure 1. A. Correlation plots of methylation distribution at IMRs in DGCs of six individual animals. Single animal methylation distribution at IMR CpGs highly correlate with that of IMR CpGs from pooled samples (r^2=0.89-0.90), suggesting intermediacy in methylation at IMRs is not due to inter-animal differences in pooled samples. Individual profiles are also highly similar to each other (r^2=0.93-0.94). **B**. CpGs outside of IMRs exhibit the expected bimodal distribution in methylation. **C,D.** IMRs are present in hippocampal CA neurons. Methylation distribution of IMR and non-IMR CpGs in CA1 (**C**) and CA3 (**D**) pyramidal cells at developmental time points E17.5 and adulthood in males**. E**. Distribution of hydroxymethylated CpGs in IMR and non-IMR regions are comparable. **F.** Density plot showing methylation distribution of 5hmC containing IMRs. BS: 5hmC+5mC (pink) and oxBS: 5mC (blue). Methylation distribution of hydroxymethylated IMRs retains IM after removal of 5hmC sites.

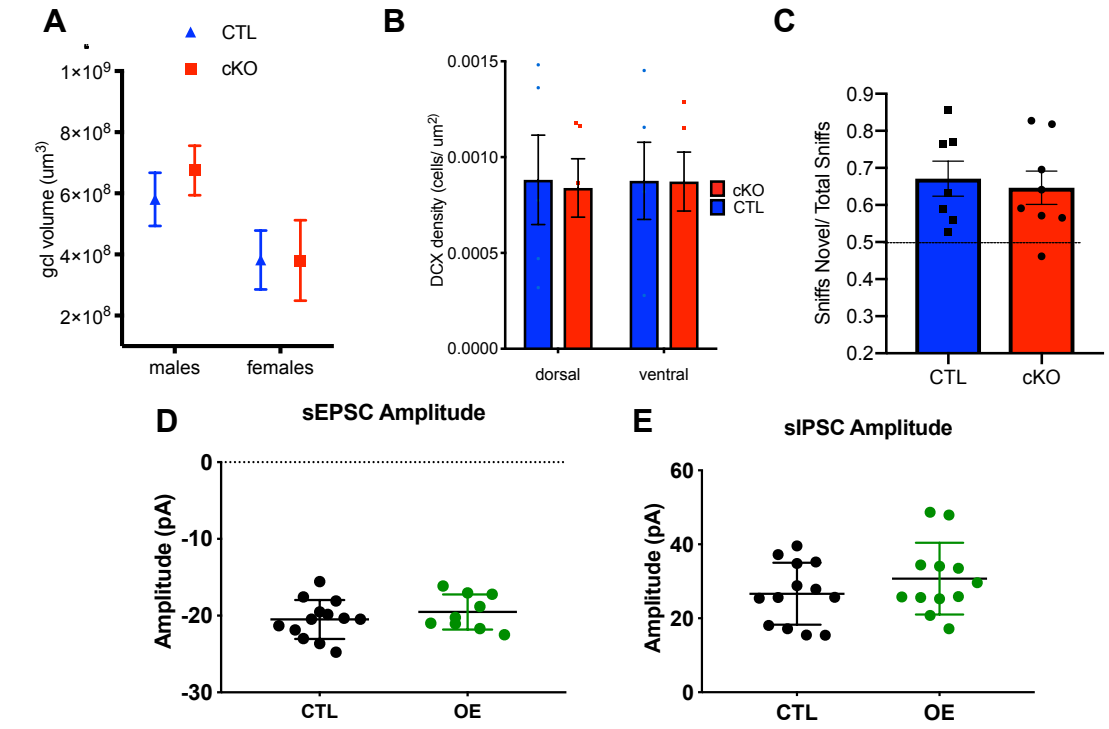

Supplemental Figure S2: DNMT3A cKO and OE cause no alterations in DG morphology, neurogenesis, and synaptic transmission. Related to Figures 3 and 4. **A**. cKO of *Dnmt3a* did not alter granule cell layer (gcl) volume. *t*-test: males, t(6)=0.8915, p=0.406992, n=4,4; females, t(8)=0.01098, p=0.991509, n=4,6. **B**. Comparable adult neurogenesis, assessed as density of DCX positive young cells in the gcl of adult cKO and control male mice. Multiple *t*-tests: dorsal t(8)=0.1535, p=0.881, n=5,5 mice, ventral t(8)=0.01532, p=0.988, n=5,5 mice. **C**. cKO mice performed similar to controls in novel object preference task. Ratio of sniffs to novel to total sniffs (novel object sniffs + habituated object sniffs). Both control and cKO mice show novel object preference above chance. One sample *t*-test, control, t(1)=3.611, **p*=0.0112, cKO, t(1)=3.243, **p*=0.0142. There was no difference in control and cKO performance. Welch-corrected *t*=0.3756, *p*=0.7133, n=6,8. **D,E.** Amplitude of spontaneous EPSCs and IPSCs were not significantly different in OE and control DGCs, indicating no detectable change in excitatory or inhibitory synaptic transmission (N=control:14 cells/7 mice, OE:17 cells/6 mice).

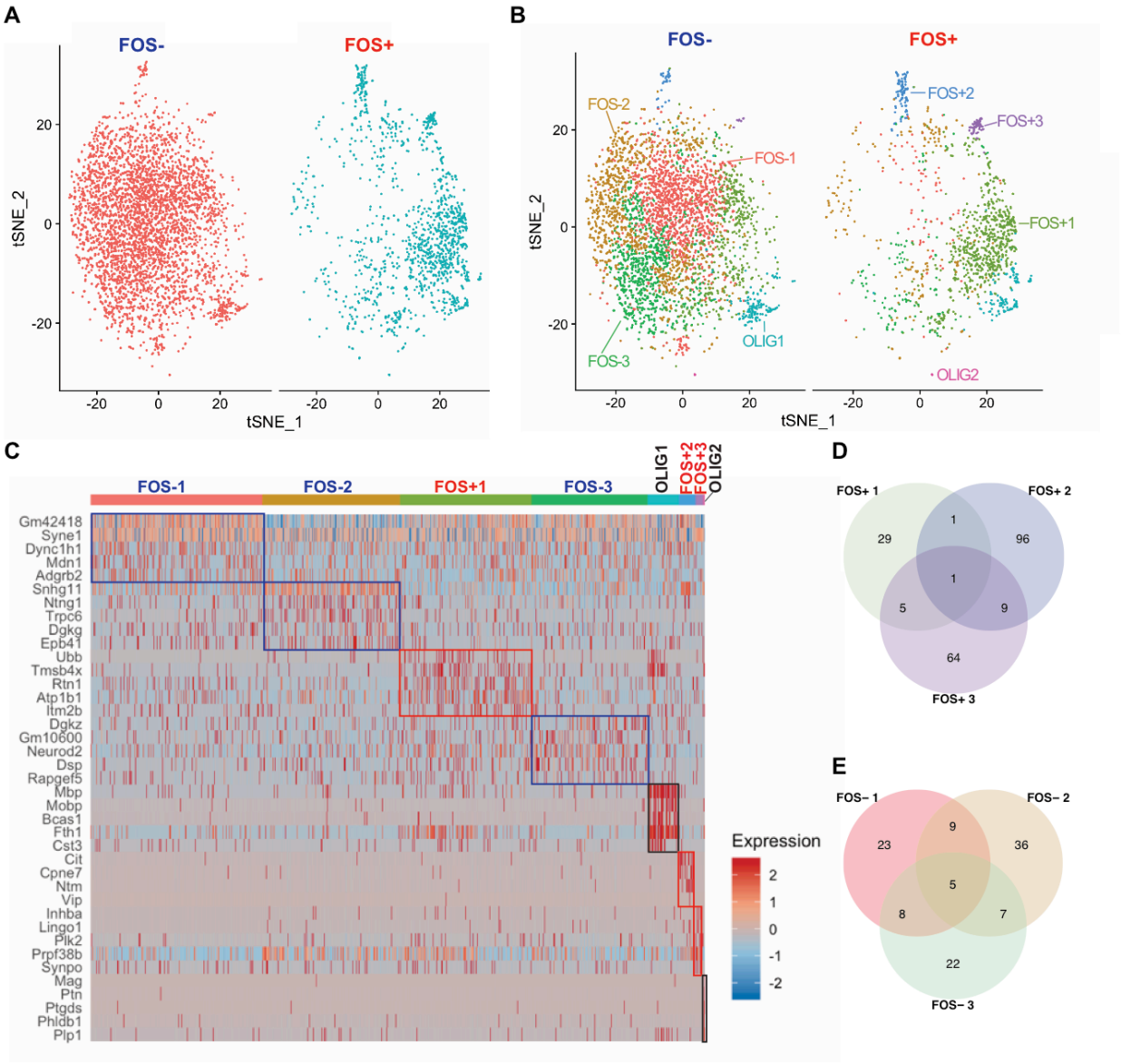

Supplemental Figure S3: Differentially expressed (DE) genes in FOS+and FOS-cell nuclei. Related to Figure 5. A,B. Sequencing data from single FOS$^+$ and FOS$^-$ cell nuclei, pooled for unsupervised cluster analysis based on differential gene expression. t-SNE plots, color coded based on FOS expression. FOS$^+$ and FOS$^-$ cells segregated from each other (A). FOS$^+$ and FOS$^-$ cells could be subdivided to three groups each, FOS$^+$1-3 and FOS$^-$1-3 (B). Two small subclusters of oligodendrocytes were also identified (Oligo1,2). **C**. Expression of the top 5 genes based on logFC in each subcluster plotted as a heatmap. **D**. The three FOS$^+$ subclusters were easily distinguishable from each other by specific sets of DE genes (adjusted p<0.05). While the largest population of FOS$^+$ nuclei, FOS$^+$1, was enriched in genes related to protein synthesis/turnover (IPA *p*=9.57E-5; *Ubb, Hsps*, *Eef1a1*, *Atp1b1*), the much smaller FOS$^+$2 and FOS$^+$3 populations were prominently represented by CREB pathway genes (*p*=1.73E-9; *Cacna1b/1e/1g, Cacng2, Camk2a/b, Gria4, Grin2d*) and synaptogenesis genes (*p*=1.07E-4; *Bdnf, Ntrk2, Nrxn2, Nrp1, Sympo, Arc, Homer1, Shank1*). **E**. In contrast, the three FOS$^-$ subclusters (with a smaller number of DE genes) shared the biological functions of synaptogenesis and calcium signaling (*p*=3.32E-4-6.44E-3 and *p*=9.09E-3, respectively).

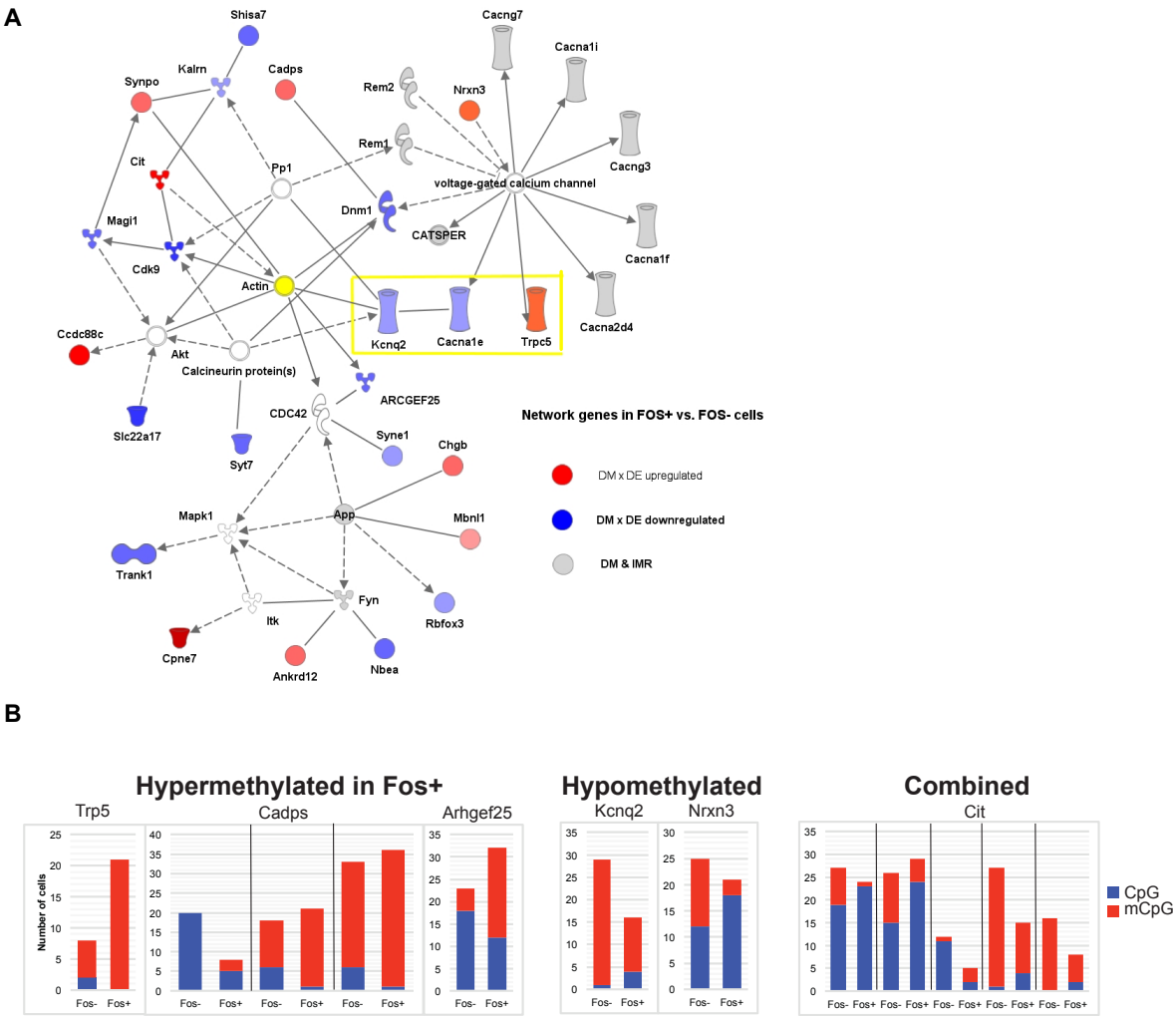

Supplemental Figure S4: Sn-methylomes and transcriptomes of activated DGCs reveal a common functional gene network. Related to Figure 5. A. Three-quarters of DM x DE genes (Figure 5K) are clustered to a gene network. In this gene network, voltage gated channels, which modulate neuronal excitability (Helbig et al., 2019; Niday et al., 2017; Phelan et al., 2013), were prominently represented (*Kcnq2, Trpc5, Cacna1e*). The network also included a gene encoding a calcium activated protein (*Cadps*), and a number of additional calcium channel genes that contained IMRs but were not DE (*Cacna1f, Cacna1l, Cacna2d4, Cacng3, Cacng7, Catsper 1,2,* and *4*). The prominence of calcium related genes in the network is in agreement with the reported role of CREB, a cAMP/Ca^{2+}activated protein, in neuronal recruitment (Han et al., 2007; Zhou et al., 2009). Another group of DE X DM genes were related to small GTPase regulatory pathways (*Archgef25*, *Kalm, Cit, Magi1, and Synpo)* which are known to regulate neurite/dendritic morphogenesis and plasticity, via actin and cytoskeletal proteins (Forrest et al., 2018). Finally, the network contained genes encoding pre- and postsynaptic proteins (*Nrx3, Kalrn, Syt7*). Interestingly, we found no DE x DM genes specific for glutamate transmission, suggesting a network function related to neuronal responsiveness to synaptic input, rather than to glutamatergic synaptic plasticity. **B**. Epiallelic frequencies in FOS-DM CpGs of representative DM X DE genes in FOS^{+} and FOS^{-} cells that are embedded in channels, cytoskeletal regulators, and cell-to-cell contact proteins.